FEBS Letters 345 (1994) 181–186

FEBS 14046

The formation of symmetrical GroEL–GroES complexes in the presence of ATP

Oscar Llorca, Sergio Marco, José L. Carrascosa, José M. Valpuesta*

Centro Nacional de Biotecnología, CSIC, universidad Autónoma de Madrid, 28049 Madrid, Spain

Received 24 March 1994

Abstract

The incubation of chaperonins cpn60 (GroEL) and cpn10 (GroES) from *E. coli* in the presence of Mg-ATP and KCl generates the formation, as revealed by electron microscopy, of GroEL–GroES complexes with a symmetrical shape in which one toroidal GroES oligomer is bound to each end of the tetradecameric GroEL aggregate (1:2 GroEL:GroES oligomer molar ratio). The symmetrical complexes are not observed in the presence of ADP or the non-hydrolyzable ATP analog, ATPγS, where only asymmetrical complexes (1:1 GroEL:GroES oligomer molar ratio) are formed. These results suggest that ATP hydrolysis is required for the formation of symmetrical complexes.

Key words: Chaperonin; GroEL–GroES complex; Protein folding; Electron microscopy; Image processing

1. Introduction

Chaperonins are members of the Hsp60 proteins involved in the proper folding and assembly of a variety of proteins [1–4]. The family comprises chaperonins of bacterial origin, like GroEL [5,6], from eukaryotic organelles, such as the mitochondrial Hsp60 [7] or the rubisco binding protein [8], from the eukaryotic cytosol, such as the TCP-1 chaperonin [9], or from thermophilic bacteria, such as TF55 from *Sulfolobus shibatae* [10]. The best known member of this family is GroEL from *E. coli*. GroEL is a 14-mer double toroid of approx. 800 kDa [5,6] which exhibits a low ATPase activity [6], requiring potassium ions [11], and this activity is inhibited in the presence of the co-chaperonin, GroES, a small heptameric ring of 70 kDa [12,13]. GroEL (from now on we will refer to GroEL and GroES as the tetradecameric and heptameric aggregates, respectively) has been found to catalyze the folding of certain proteins in an Mg-ATP-dependent manner [14,15]. For the folding of other proteins, Mg-ATP and GroES are needed [14,16]. GroES seems to modulate the function of GroEL by coupling the K^+-dependent hydrolysis of ATP to the exit from GroEL of the folded or partially folded target protein [11]. According to the most recently proposed mechanism, GroES stabilizes GroEL in the ADP-bound state. Binding of the unfolded protein within the GroEL cavity triggers ADP and GroES exit. Upon exchange of ADP for ATP, GroES binds again to GroEL and the hydrolysis of ATP releases the bound protein for folding. Partially folded protein can repeat this charge–discharge cycle until folding is complete [17].

Using both electron microscopy and biochemical techniques, GroES has been found to form a 1:1 asymmetric complex with GroEL by binding to one end of the GroEL double toroid [18,19]. The binding of GroES would trigger conformational changes in the other end of GroEL so that the binding of another GroES is apparently impeded [19]. Here we describe the formation of symmetrical GroEL–GroES complexes, with a ring of GroES on each side of the GroEL oligomer (GroEL:GroES, 1:2), as opposed to the already described asymmetrical 'bullet-shaped' complexes (GroEL:GroES, 1:1). This result is discussed in the light of new data on the ATPase activity of GroEL in the presence of GroES [20].

2. Materials and methods

2.1. Purification of GroEL and GroES

E. coli chaperonins were obtained from a pOF39 plasmid-harbouring *E. coli* strain that over-expresses both GroEL and GroES [21]. Cells were lysed with alumina at 4°C and suspended in buffer A (50 mM Tris-HCl, 2 mM EDTA, 0.02% NaN_3, pH 7.7). The lysate was centrifuged at 15,000 × *g* for 30 min at 4°C. Supernatant was mixed with 0.4 M NaCl in buffer A (1:10, supernatant/buffer volume ratio) and precipitated with 1% polyethylenimine (final concentration) for 30 min at 4°C. After centrifugation at 15,000 × *g* for 30 min at 4°C, supernatant and pellet were separated. Pellet contained GroEL while supernatant contained GroES, and, therefore, they were purified separately.

The GroEL-containing precipitate was extracted overnight with 1 M NaCl in buffer A at 4°C. Supernatant was precipitated with 60% ammoniun sulfate and then centrifuged in a 5–20% sucrose gradient at 415,000 × *g* for 2.5 h at 4°C [22]. Fractions were analysed by SDS-PAGE [23]. The fractions containing pure GroEL were pooled and stored at −80°C. The GroES-containing supernatant was precipitated with 55% saturated ammonium sulfate. The precipitate was re-dissolved in a small volume of buffer A and dialysed overnight against the same buffer (10-fold) at 4°C. After centrifugation at 15,000 × *g* for

*Corresponding author. Fax: (34) (1) 585 4506.
E-mail: jmv@samba.cnb.uam.es

SSDI 0014-5793(94)00432-U

30 min at 4°C, the GroES-enriched supernatant was loaded onto a hydroxylapatite column (Calbiochem) previously equilibrated with buffer A. GroES was eluted with a 5–90 mM potassium phosphate gradient. Fractions were analysed by SDS-PAGE and the fractions containing GroES were pooled and dialysed overnight against buffer A with 50 mM NaCl. The resulting solution was then applied onto a DEAE-32 column (Whatman) equilibrated with 50 mM NaCl in buffer A and eluted with a 50–300 mM NaCl gradient in the same buffer. Fractions containing pure GroES were pooled and stored at −80°C. GroES was more than 95% homogeneous as revealed by SDS-PAGE.

2.2. Rhodanese refolding assay

Rhodanese from bovine liver (Sigma) was denatured in 8 M guanidinium chloride and diluted 50-fold into buffer 50 mM Tris-HCl containing 0.2 μM GroEL, 0.3 μM GroES, 2 mM ATP, 15 mM $MgCl_2$, 5 mM KCl, 1 mM DTT and 70 mM $Na_2S_2O_3$. Rhodanese final concentration was 0.35 μM. Incubation was carried out at 37°C. Controls omitting one of the chaperonins or the ATP were made to determine rhodanese refolding requirements. Rhodanese activity was measured as described [24]. 50 μl aliquots were removed from the incubation mixture at 0, 15, 30 and 60 min. 10 μl of 0.5 M EDTA was added to each aliquot to stop the Mg-ATP-dependent chaperonin reaction. Aliquots were then added to the standard assay mixture and the reaction product was determined after 30 min incubation at 37°C.

2.3. Sample preparation and electron microscopy

GroEL (0.3 μM, final concentration) samples were incubated for 15 min at room temperature in 50 mM Tris-HCl, 15 mM $MgCl_2$, 5 mM KCl and 2 mM ATP at pH 7.7 (final concentrations). GroEL–GroES complexes (1:1.5 and 1:5 oligomer molar ratio) were prepared by mixing GroE and GroES in 50 mM Tris-HCl, pH 7.7, 10 mM $MgCl_2$, 5 mM KCl and 2 mM ATP, 2 mM ADP or 2 mM ATPγS (Boehringer) in each case (final concentrations). Complexes were incubated for 15 min at room temperature. GroEL and GroEL–GroES complexes were negatively stained with freshly made 2% uranyl acetate on thin carbon-coated collodion grids previously glow-discharged for 15 s. Transmission electron microscopy was performed in a JEOL 1200EX electron microscope operated at 100 kV. Electron micrographs were obtained under minimum electron dose conditions at a magnification of × 60,000 on KodaK film SO-163.

2.4. Image processing

Micrographs were digitized using a Eikonix IEEE-488 camera with a pixel size equivalent to 0.7 nm in the specimen plane. All particle projections corresponding to side views were selected. Then, 64 × 64 pixel single particles were extracted and translationally aligned by cross-correlation with a circular mask. Population homogeneity was tested by means of a neural network self-organizing Kohonen-based map classifier [25,26]. When different populations were observed in the classification map, each homogeneous groups was processed independently to obtain an average image using a reference-free alignment method [22,27]. Resolution was estimated by the spectral signal-to-noise ratio (SSNR) method [28].

3. Results and discussion

3.1. Characterization of functional assay conditions

Due to the complexity of the interaction of the different factors involved in the process of protein folding mediated by chaperonins, we focused our attention on a simple assay that measures the folding of rhodanese in the presence of GroEL and GroES [19,24]. Both proteins, purified as described in section 2, are required for the succesful folding of rhodanese in the presence of 2 mM ATP and 15 mM $MgCl_2$ (Fig. 1). We then studied the morphology of the chaperonin complexes formed under these conditions that led to active peptide folding.

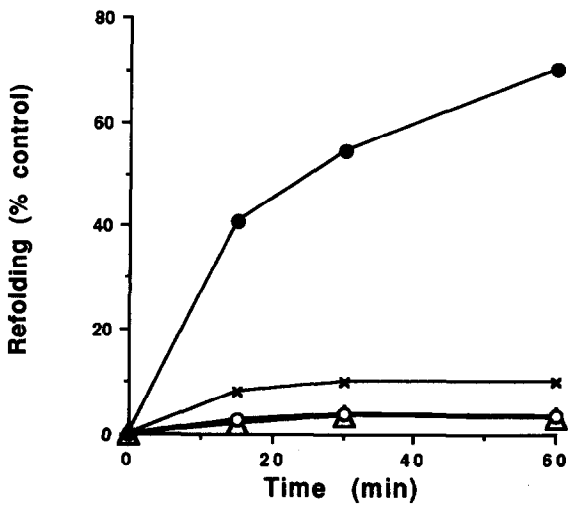

Fig. 1. Rhodanese refolding assay. Rhodanese was unfolded and refolded as described in section 2. Refolding was carried out in the presence of GroEL, GroES and Mg-ATP (●), GroEL and Mg-ATP (○), GroES and Mg-ATP (×) or GroEL and GroES without ATP (△). The final concentration of rhodanese in the mixture was 0.37 μM. Rhodanese refolding is expressed as a percentage of the activity obtained for 0.37 μM native non-denatured rhodanase under the same conditions.

3.2. Structure of the GroEL–GroES complexes built up in the presence of ATP

The interaction of GroEL and GroES in the presence of ADP leads to the formation of an asymmetric complex in which the GroES seems to interact with only one of the two ends of the cylindrically shaped GroEL [18,19,29]. This interaction also induces a number of changes in the morphology of GroEL, some of them similar to those produced by the interaction of GroEL with ATP [29]. Electron microscopy of the complexes formed under the conditions of the functional assay described in Fig. 1 showed, besides the characteristic circular front views, the presence of side views that were clearly different to those found in the absence of GroES (Fig. 2A,B). Besides the so called 'bullet-shaped' side views that have been described previously (Fig. 2B, arrowheads), other images were consistently found that showed more symmetrical profiles than the former (Fig. 2B, arrows). While at a 1:1.5 GroEL:GroES molar ratio the symmetrical particles represented 50% of the total GroEL–GroES complexes, they reached 95% at a 1:5 GroEL:GroES molar ratio.

In an attempt to distinguish classes among the observed side views from the complexes, the population was subjected to a Kohonen-based self-organizing map [25,26]. Fig. 3 shows the presence of representative side views that are either symmetrical (labeled S) or asymmetrical (labeled A). To further analyze these views, images corresponding to each class were averaged (Fig. 4).

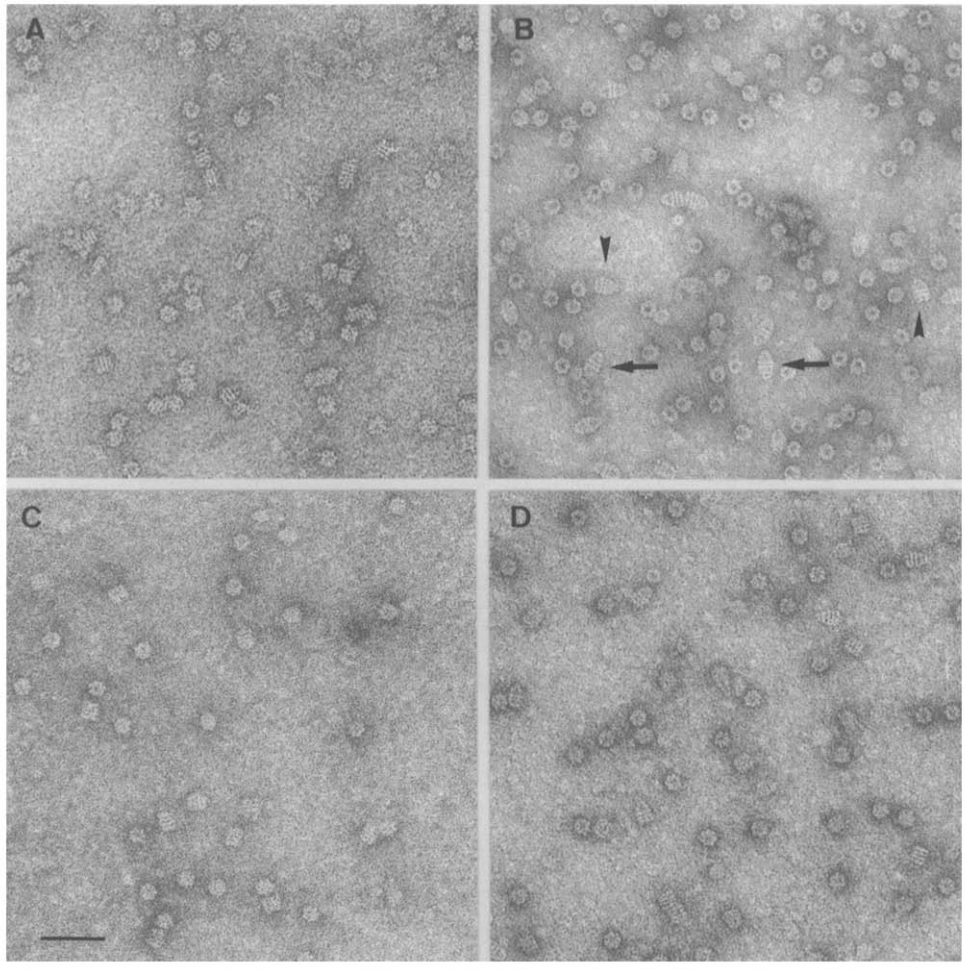

Fig. 2. Representative fields of micrographs resulting from the incubation of (A) GroEL with Mg-ATP and K^+, (B) GroEL, GroES, Mg-ATP and K^+, (C) GroEL, GroES, Mg-ADP and K^+, and (D) GroEL, GroES, Mg-ATPγS and K^+. In B two structural classes of side views are observed, aparently corresponding to previously described asymmetric GroEL–GroES complexes (arrowheads) and to more symmetrical complexes (arrows). In C and D only asymmetrical complexes and non-bound GroEL could be seen. Bar = 50 nm.

Asymmetrical side views were consistent with those previously described [18,19], with the additional mass (most likely corresponding to GroES) clearly visible at one end of the GroEL cylinder (Fig. 4A,B). On the other hand, the other views are quite symmetrical, with two similar regions at both ends of the rectangular projection of the GroEL cylinder. The acceptable resolution of these averages (2–3 nm) allowed a close comparison between them, revealing the similarity of the caps in both the symmetrical and asymmetrical complexes (Fig. 4C), with the rest of the structure being very similar to the already described complexes. The morphology of the symmetrical GroEL–GroES complex is consistent with the hypothesis that these particles result from the interaction of one GroES toroid at each end of the GroEL cylinder.

3.3. *Structure of the GroEL–GroES complex formed in the presence of ADP and non-hydrolizable ATP*

The surprising finding of GroEL aggregates capped at both ends with two GroES toroids in the presence of ATP and magnesium posed the question of the eventual role of these complexes in the chaperonin-mediated folding mechanism. As a first step, we checked whether ATP was strictly needed for the formation of the symmetric complex. GroEL and GroES were incubated under the conditions described for the functional assay, except that ADP was added instead of ATP. Electron microscopy of the samples revealed side views corresponding to the asymmetric class (Fig. 2C), that after averaging (Fig. 5A) were similar to the asymmetrical ones found under ATP incubation (Fig. 4B) or those previously described [18,19].

Due to the absence of symmetric views in the presence of ADP, samples of GroEL and GroES were incubated in the presence of the non-hydrolyzable ATP analog, ATPγS [30]. No symmetrical complexes were observed in those preparations (Fig. 2D). The averaged image of the asymmetric complex found under these conditions

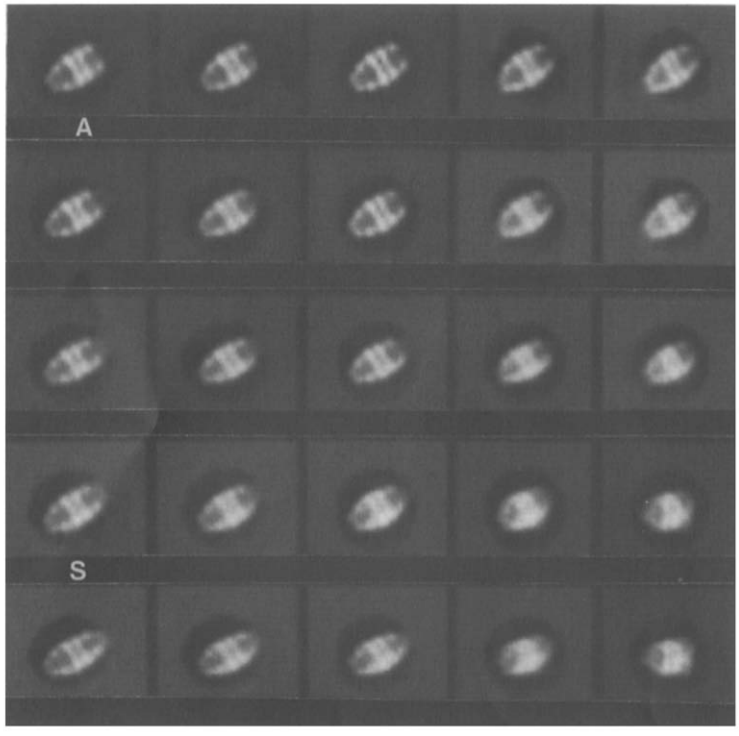

Fig. 3. Dictionary output vectors corresponding to a Kohonen-based image classification of side views obtained from samples of GroEL and GroES incubated in the presence of Mg-ATP and K^+. Two clearly different GroEL–GroES complexes are located at opposite corners in the classification map. The top left-hand corner shows asymmetrical complexes (labeled A) while the bottom left-hand corner corresponds to symmetrical complexes (labeled S).

was essentially identical to that found using ADP (Fig. 5B).

A common structural feature in the asymmetric complexes found with ADP and ATPγS is the fact that the GroEL end distal to the one interacting with GroES is different to the one found in the complexes obtained after ATP incubation (compare Figs. 4B, 5A, and 5B). Although the difference is subtle, it is clear that in the complex formed with ATP, both GroEL ends are more similar (i.e. following a truncated cone profile, as described for the isolated GroEL incubated with ATP [29]), whereas in the asymmetrical complexes formed in the presence of ADP or ATPγS, the end distal to the one interacting with GroES is more similar to the flat cylinder end characteristic of the GroEL devoid of ATP. Due to the fact that differences in this range have been described already as possible classes reflecting an intrinsic structural heteronegeity of GroEL–GroES complexes

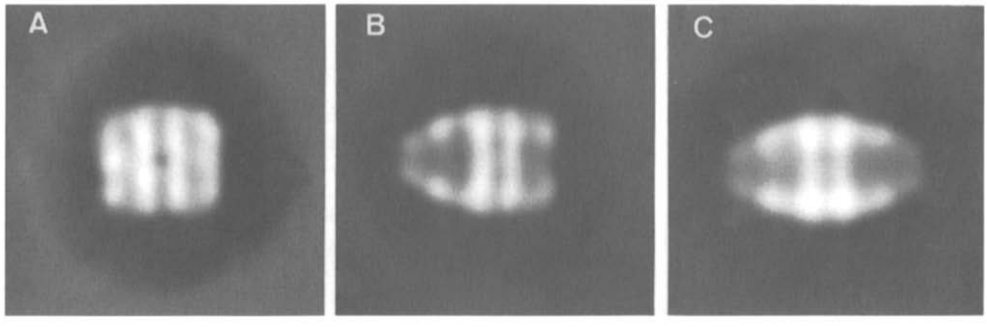

Fig. 4. Average projection images of GroEL and GroEL–GroES complexes obtained after incubation in the presence of Mg-ATP and K^+. (A) Average side view from negatively stained GroEL. The length and width of the average image is 15 nm and 13 nm, respectively. (B) Average side view from asymetrical complexes. This average is consistent with one GroES asymmetrically bound to just one end of the GroEL double toroid. The length and width of the average image is 18.5 nm and 13 nm, respectively. (C) Average side view from symmetrical complexes. The length and width of the average is 21.7 nm and 13 nm, respectively. This average image is consistent of GroES binding simultaneously to both ends of the GroEL double toroid. The total number of particles used in the final average image were 237, 912 and 421, respectively. The final resolution obtained was 3.1 nm, 2.3 nm and 2.8 nm, respectively.

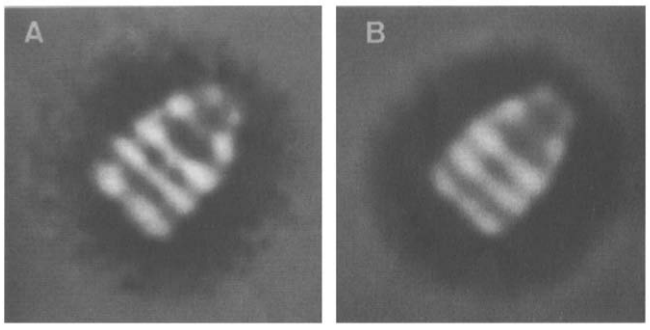

Fig. 5. Average side views of GroEL–GroES complexes obtained after incubation in the presence of K^+ and (A) Mg-ADP and (B) Mg-ATPγS. Only asymmetrical GroEL–GroES complexes were observed in both cases. The total number of particles used in the final average image was 169 and 102, respectively. The final resolution obtained was 3.0 nm and 3.2 nm, respectively.

[19], the real significance of these differences between ATP, ADP and non-hydrolizable ATP demand further analysis of more numerous particle populations to yield higher resolution and to allow better classification procedures.

Most of the current models for the chaperonin-assisted folding mechanism are based on reaction cycles that involve the sequential interaction of GroEL and GroES correlating with cycles of ATP binding and hydrolysis [17,20]. All these models rely on the functionality of asymmetric GroEL–GroES complexes where one GroES complex binds to one end of the GroEL cylinder, although both ends are potentially capable of binding GroES [17,31,32]. The finding that GroES can be assembled at both ends of the GroEL cylinder under functional conditions poses the question of a possible role of this complex in the folding mechanism. Binding of one GroES toroid to one GroEL oligomer gives rise to a decrease in the ATP hydrolysis to 50% of the GroEL rate [33]. Furthermore, there is a subsequent step in which the ATP hydrolysis is completely inhibited, a step that can be reversed, increasing the ATP/ADP ratio [20]. One evident explanation for this change from 50% hydrolysis to a total inhibition could be the interaction of a second GroES toroid to the asymmetric GroEL–GroES complex, thus leading to a symmetrical inhibited complex that would have to be taken into account when describing the folding cycle (an hypothesis already suggested in [20]).

The fact that symmetrical complexes are only present under conditions leading to folding activity, and not when ADP is used, explains why they have not been detected in previous studies [19,29]. On the other hand, the absence of these symmetrical complexes when the incubation is carried out with a non-hydrolizable ATP homolog suggest that ATP hydrolysis might be needed to generate a stable complex, and further supports the possible functional relevance of these symmetrical complexes.

Although additional studies will be needed to clarify the role of the symmetrical complex in the chaperonin-assisted folding mechanism of peptides, as well as its relationship with the GroEL complex and the asymmetric GroEL–GroES complex, the results presented in this paper will drive other studies looking for these new complexes in different experimental systems and under other experimental conditions.

Acknowledgements: This work was partially supported by grant PB91-0109 from the Dirección General de Investigación Científica y Técnica. O.L. is a fellow from the Gobierno de Navarra and S.M. is a fellow from the Comunidad Autónoma de Madrid.

References

[1] Gatenby, A.A. and Ellis, R.J. (1990) Annu. Rev. Cell Biol. 6, 125–149.
[2] Ellis, R.J. and van der Vies, S.M. (1991) Annu. Rev. Biochem. 60, 321–347.
[3] Zeilstra-Ryalls, J., Fayet, O. and Georgopoulos, C. (1991) Annu. Rev. Microbiol. 45, 301–325.
[4] Gething, M.J. and Sambrook, J. (1992) Nature 355, 33–45.
[5] Hohn, T., Hohn, B., Engel, A., Wurtz, M. and Smith, P.R. (1979) J. Mol. Biol. 129, 359–373.
[6] Hendrix, R. (1979) J. Mol. Biol. 129, 375–392.
[7] Viitanen, P.V., Lorimer, G.H., Seetharam, R., Gupta, R.S., Oppenheim, J., Thomas, J.O. and Cowan, N.J. (1992) J. Biol. Chem. 267, 695–698.
[8] Barraclough, R. and Ellis, R.J. (1980) Biochim. Biophys. Acta 608, 19–31.
[9] Gao, Y., Thomas, J.O., Chow, R.L., Lee, G.-H. and Cowan, N.J. (1992) Cell 69, 1043–1050.
[10] Trent, J.D., Nimmesgern, E., Wall, J.S., Hartl, F.U. and Horwich, A.L. (1991) Nature 354, 490–493.
[11] Viitanen, P.V., Lubben, T.H., Reed, J., Goloubinoff, P., O'Keefe, D.P. and Lorimer, G.H. (1990) Biochemistry 26, 5665–5671.
[12] Chandrasekhar, G.N., Tilley, K., Woolford, C., Hendrix, R. and Georgopoulos, C. (1986) J. Biol. Chem. 261, 12414–12419.
[13] Weaver, A.J., Landry, S.J. and Deisenhofer, J. (1993) Biophys. J. 64, A350.
[14] Buchner, J., Scmidt, M., Fuchs, M., Jaenicke, R., Rudolph, R., Schmid, F.X. and Kiefhaber, T. (1991) Biochemistry 30, 1586–1591.
[15] Martin, J., Langer, T., Boteva, R., Schramel, A., Horwich, A.L. and Hartl, F.U. (1991) Nature 352, 36–42.
[16] Goloubinoff, P., Christeller, J.T., Gatenby, A.A. and Lorimer, G.H. (1989) Nature 342, 884–889.
[17] Martin, J., Mayhew, M., Langer, T. and Hartl, F.U. (1993) Nature 366, 228–233.
[18] Saibil, H.R., Dong, Z., Wood, S. and auf der Mauer, A. (1991) Nature 353, 25–26.
[19] Langer, T., Pfeifer, G., Martin, J. Baumeister, W. and Hartl, F.U. (1992) EMBO J. 11, 4757–4765.
[20] Todd, M.J., Viitanen, P.V. and Lorimer, G.H. (1993) Biochemistry 32, 8560–8567.
[21] Fayet, O., Louarn, J.M. and Georgopoulos, C. (1986) Mol. Gen. Genet. 202, 435–445.
[22] Carrascosa, J.L., Abella, G., Marco, S. and Carazo, J.M. (1990) J. Struct. Biol. 104, 2–8.
[23] Laemmli, U.K. (1970) Nature 227, 680–685.

[24] Westly, J. (1981) Methods Enzymol. 77, 285–291.
[25] Kohonen, T. (1990) Proc. IEEE 78, 1464–1480.
[26] Marabini, R. and Carazo, J.M. (1994) Biophys. J. (in press).
[27] Penczek, P., Radermacher, M. and Frank, J. (1992) Ultramicroscopy 40, 33–53.
[28] Unser, M., Trus, B.L. and Steven, A.C. (1987) Ultramicroscopy 23, 39–52.
[29] Saibil, H.R., Zheng, D., Roseman, A.M., Hunter, A.S., Watson, G.M.F., Chen, S., auf der Mauer, A., O'Hara, B.P., Wood, S.P., Mann, N.H., Barnett, L.K. and Ellis, R.J. (1993) Curr. Biol. 3, 265–273.
[30] Bochkareva, E.S., Lissin, N.M., Flyn, G.C., Rothman, J.E. and Girshovich, S. (1992) J. Biol. Chem. 267, 6796–6800.
[31] Burns, D.L., Kessel, M., Arciniega, J.L., Karpas, A. and Gould-Kosta, J. (1992) J. Biol. Chem. 267, 25632–25635.
[32] Cejka, Z., Gould-Kosta, J. Burns, D. and Kessel, M. (1993) J. Struct. Biol. 111, 34–48.
[33] Jackson, G.S., Staniforth, R.A., Halsall, D.J., Atkinson, T., Holbrook, J.J., Clarke, A.R. and Burston, A.R. (1993) Biochemistry 32, 2554–2563.